Nanogratings Embedded in Al_2O_3-Dy_2O_3 Glass by Femtosecond Laser Irradiation

Satoshi Mori[1], Torataro Kurita[1], Yasuhiko Shimotsuma[*1], Masaaki Sakakura[2] and Kiyotaka Miura[1]

[*1] *Department of Material Chemistry, Graduate School of Engineering, Kyoto University, Kyoto, 615-8510, Japan*
E-mail: yshimo@func.mc.kyoto-u.ac.jp
[2] *Office of Society-Academia Collaboration for Innovation, Kyoto University, Kyoto, 615-8510, Japan*

The self-assembled nanogratings embedded in number of materials, which are aligned according to the laser polarization, is an intriguing phenomenon induced by femtosecond light pulses. Curiously, the orientation of such periodic nanostructure is different between a glass and an indirect bandgap semiconductor. Furthermore a material in which nanogratings can be induced is limited. Here we report that a polarization-dependent periodic nanostructure can be successfully induced in Al_2O_3-Dy_2O_3 binary glass with a low glass formation ability. In the case of this binary glass, we confirmed that the self-organization and partial-crystallization were simultaneously induced by the laser irradiation. Such photoinduced structure in Al_2O_3-Dy_2O_3 glass exhibit periodic modulation in magnetic properties in nanoscale.
DOI: 10.2961/jlmn.2016.01.0016
Keywords: femtosecond laser, self-organization, nanostructure, aerodynamic levitation, magnetic properties

1. Introduction

1.1 Self-assembled subwavelength nanostructure

One of the intriguing phenomena induced by the femtosecond laser pulses is the formation of the polarization-dependent subwavelength nanostructure [1]. In the case of SiO_2 or GeO_2 glass, nanograting structures, which are composed of stripe-like regions with oxygen deficiencies including nanovoids [2], are aligned perpendicular to the laser polarization [3]. Since the discovery of the laser-induced periodic surface structure (LIPSS) by Birnbaum nearly a half-century ago [4], many interesting researches have been carried out from the experimental [5] and theoretical [6] perspectives. As opposed to the laser-induced periodic surface structure (LIPPS) on the various materials (metal, semi-conductor, dielectrics), nanogratings inside of the material were found only for handful materials [7, 8]. The formation mechanism of nanogratings is also still a mystery [1, 9]. Since the subwavelength stripe-like regions of lower oxygen concentration including nanovoids exhibit lower density, the optical anisotropy in form birefringence can be induced in the isotropic material, namely glass [10]. Based on such photoinduced structures showing localized birefringence in glass, various application ranging from embedded microreflectors [11], retardation plates [12], microfluidic channels [13], to rewritable 5D optical storage [14], polarization imaging [15] have been investigated [16]. It should be noted that the self-organization phenomenon of highly oriented subwavelength nanostructure can be observed in few glass material of usual glass-forming oxides such as SiO_2 and GeO_2. In this paper, we prepared Al_2O_3-Dy_2O_3 binary glass which is not containing network-former (e.g. SiO_2, GeO_2) using aerodynamic levitation with CO_2 laser heating. Since Dy concentration is very high, this glass has a property of sticking to a magnet.

1.2 Aerodynamic levitation with CO_2 laser heating

Aerodynamic levitation melting method is one of the containerless melting methods. Since the mixture of raw materials can be melted in the containerless state, a heterogeneous nucleation from the container walls is prevented. As the result, deeply supercooled state is realized, and it is possible to form glass in compositions which essentially are not vitrifiable [17]. The binary Al_2O_3-based [18, 19], TiO_2-based [20, 21] and Nb_2O_5-based [22, 23] composition glasses have been investigated by using containerless processing method. More recently, Watanabe et al. reported that the binary R_2O_3-Al_2O_3 glass (R is a rare earth element) can be formed by using aerodynamic levitation furnace method.

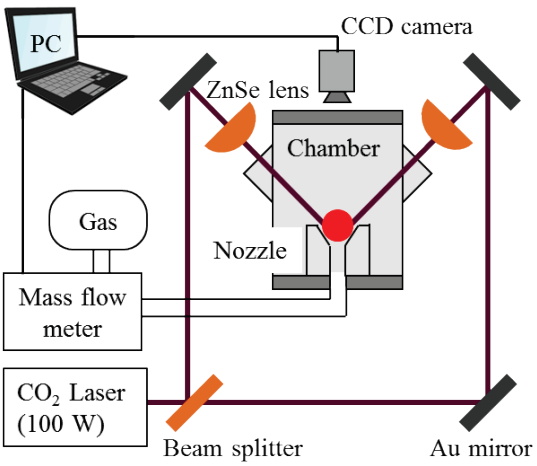

Fig. 1 Schematic of aerodynamic levitation with CO_2 laser heating furnace.

2. Experimental

2.1 Al_2O_3-Dy_2O_3 binary glass preparation

Aluminum oxide and dysprosium oxide raw powders with a composition of $70Al_2O_3$-$30Dy_2O_3$ were mixed in alumina mortar and pressed into pellets, and then the pellets were sintered for 12 hours at 1100 °C in air. The calcinated pellets were crushed and used as a preform for the aerodynamic levitation with CO_2 laser heating (Fig. 1). The calcinated preforms were levitated by a flow of dry air (N_2:79 % O_2:21 %) and melted by focusing of 100 W CO_2 laser via ZnSe lens (f = 254 mm). To make the melt homogeneous, the temperature was kept above melting point for dozens of seconds. And then, by turning off the laser power, the melt was rapidly cooled. A yellowish spherical sample was obtained (Fig. 2). When there were bubbles in obtained samples, they were melted again because bubbles interrupt the laser propagation. The glass phase of solidified samples were confirmed by Cu Kα X-ray diffraction (XRD; Rigaku, RINT-2500HFK/PC). The glass transition temperature (T_g) and the crystallization temperature (T_x) for as-prepared glass were determined 866 °C and 925 °C, respectively, by using differential scanning calorimetry (DSC; Rigaku, ThermoPlus2 DSC8270) with a heating rate of 10 °C/min. The samples were annealed at a temperature 5 °C higher than T_g for 1 hour to remove the residual stress. After annealing, the top and bottom parts of the spherical glass samples were polished parallel for the laser irradiation experiments. Based on the Lorentz-Lorentz relation [24], the refractive index of $70Al_2O_3$-$30Dy_2O_3$ glass was estimated to be ~1.7.

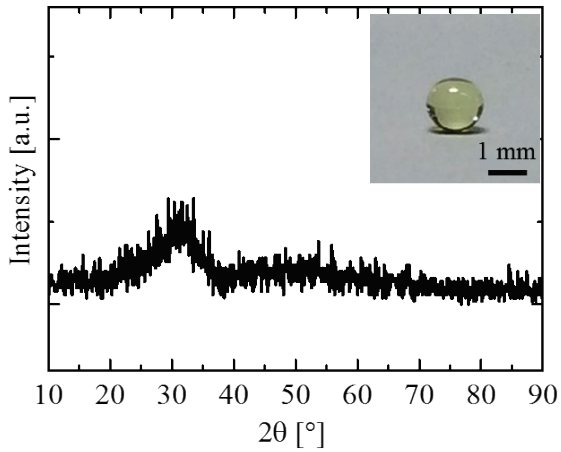

Fig. 2 X-ray diffraction pattern of the solidified sample. Inset shows a photo of the obtained $70Al_2O_3$-$30Dy_2O_3$ glass.

2.2 Femtosecond laser irradiation

We used the 50 fs laser pulses emitted from a regenerative amplified mode-locked Ti: Sapphire laser, operating at a wavelength of 800 nm with 250 kHz repetition rate. The laser pulses were focused at 100 μm below the glass sample surface via 50× microscope objective lens with a numerical aperture of 0.80. Due to the high refractive index, it should be considered that actual pulse duration at the focal point was stretched. The laser energy was controlled by a variable neutral density filter (typically, 1.0 and 1.5 μJ). Focus spot was scanned for 200 μm at 1 μm/s by moving glass sample placed on the XYZ translation stage. Simultaneously, the irradiated spot was observed using CCD camera (Toshiba-teli, CSDW2M60CM28).

2.3 Characterization of photoinduced structure

After laser irradiation, the modified region in glass samples were inspected using a conventional optical microscope and a polarization microscope (LC-Polscope). The structural changes in the glass were analyzed by a confocal Raman spectrometer excited by DPSS laser with a wavelength of 532 nm (Tokyo Instruments; NanoFinder 30). After polishing the sample to the depth of the beam waist location, the polished sample surface was also inspected using a FE-SEM (JEOL, JSM-6705F). To confirm the detailed of the photoinduced structure, we have also performed the characterization of magnetic properties using Magnetic Force Microscope (MFM; Bruker, MultiMode8).

3. Results and discussion

3.1 Optical and polarization microscope inspection

Fig. 3 shows the optical and polarization microscope images of the modified region in $70Al_2O_3$-$30Dy_2O_3$ glass after the irradiation of femtosecond laser pulses with the energy of 1.0 and 1.5 μJ. The *v* shows the scanning direction of the focus. In the polarization microscope images, the direction of slow axis is indicated by pseudo color (see polar legend in Fig. 3). Polarization microscope images indicate that the birefringence was induced by the laser irradiation. In the case of the laser energy less than 1.0 μJ, the slow axis of the induced birefringence was oriented parallel to the laser scanning direction, regardless of the polarization direction. On the other hand, in the case of laser energy greater than 1.3 μJ, the direction of the birefringence was aligned perpendicular to the polarization direction. This phenomenon is similar to the case of SiO_2 [14] and GeO_2 glass [25]. These results show that, for this glass, the threshold of the birefringence expression is at about 1.0 μJ.

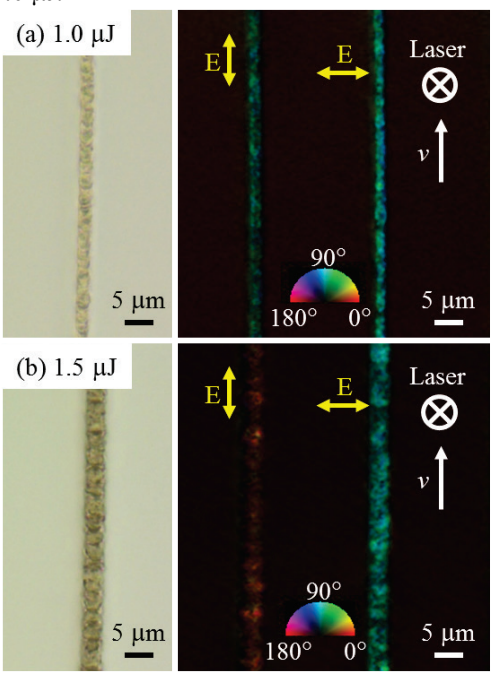

Fig. 3 Optical (left) and polarization (right) microscope images of the laser traces inside $70Al_2O_3$-$30Dy_2O_3$ glass samples written by the femtosecond laser pulses with different polarization directions and pulse energy of (a) 1.0 μJ and (b) 1.5 μJ. E and *v* show the polarization direction and the laser writing direction.

3.2 SEM observations of photoinduced structures

In the case of Al_2O_3-Dy_2O_3 binary glass, we have also confirmed that polarization-dependent periodic nanostructures were successfully formed by the femtosecond laser irradiation (Fig. 4). In both condition of 1.0 μJ and 1.5 μJ, the induced structure can be clearly observed in the backscattering electron image (BEI) although no apparent structure cannot be observed in the secondary electron image (SEI). In particular, the periodicity of the induced nanostructure for 1.0 μJ was not high. It could be interpreted in terms of overwriting of nanostructure. On the other hand, in the case of 1.5 μJ, periodic nanostructure was continuously formed along the laser writing direction. The direction of the nanograting structure with a period of about 200 nm was aligned perpendicular to the polarization direction. Such structure is similar to the induced nanostructure in SiO_2 glass. Considering the similar threshold of self-assembled nanostructure for SiO_2 glass [1], the electron plasma density and temperature in Al_2O_3-Dy_2O_3 glass during laser irradiation could be also similar to that of SiO_2 glass.

Considering the polarization-direction independent birefringence at 1.0 μJ in Fig. 3, the contribution to the photoinduced form birefringence of the intermittent nanostructures at the low energy could be low. On the other hand, we assumed that in the case of 1.5 μJ, in addition to the birefringence of nanostructures, the internal stress derived from space-selective crystallization shows larger birefringence. More detailed investigations should be required.

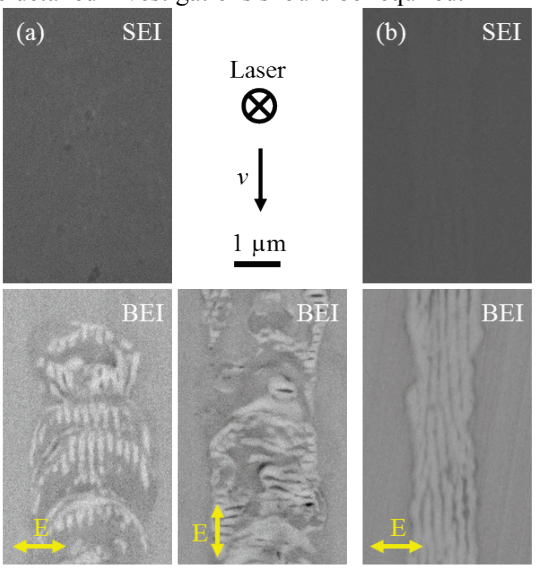

Fig. 4 SEIs (left) and BEIs (right) on the sample surface polished to the depth of laser focus. (a) 1.0 μJ, (b) 1.5 μJ. BEI for the different polarization direction at 1.0 μJ are also shown.

3.3 Raman measurements of local crystal structure

To reveal the structural changes inside glass, Raman spectra of the modified region after the laser irradiation were measured as shown in Fig. 5. Although no apparent Raman peak was observed in the initial glass, some characteristic peaks can be observed after laser irradiation. The reference Raman spectrum of the sample crystallized by heating at 870 ˚C for 24 hours in air was also shown. The crystalline phase was assigned to $Dy_3Al_2(AO_4)_3$ by XRD. The comparison of Raman spectra between the modified region and reference sample indicates the localized crystallization of $Dy_3Al_2(AO_4)_3$ in $70Al_2O_3$-$30Dy_2O_3$ glass after laser irradiation. It should be noted that no apparent changes in Raman peak position and width were observed when the laser pulse energy was changed. Fig. 6 shows Raman spectral map of typical crystalline peak at 256 cm^{-1} in glass. This result indicates that crystallization occurred in the center of the laser-writing region. Furthermore, from the results of Fig. 4 and Fig. 5, crystallization occurred simultaneously with the nanostructure formation.

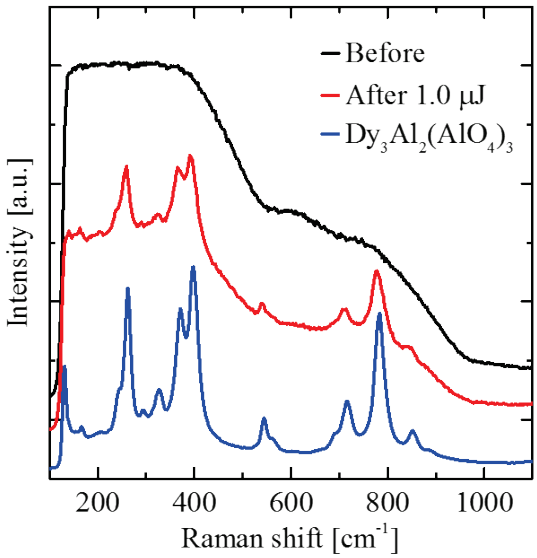

Fig. 5 Raman spectra before (black line) and after (red line) the laser irradiation at 1.0 μJ. Raman spectrum of the glass sample crystallized by heat treated was also shown (blue line).

3.4 Investigation of nanoscale magnetic properties

To reveal the local magnetic properties of the nanograting structure, the magnetic force microscope (MFM) image on the sample surface polished to the depth of focal location was observed. (Fig. 7). This MFM phase image obtained in lift mode with maintaining constant probe-surface separation. The contrast observed in the MFM image is attributed to the interaction between MFM probe and the magnetic field from the sample. As the probe moves over a magnetic field gradient, it is either pulled toward or repulsed away from the sample, depending on the magnetic moment direction. Such interactions cause a shift in phase of probe oscillation [19]. From the BEI image in Fig.4 and this MFM image, the polarization-dependent periodic nanostructures are apparently similar to the nanoscale magnetic domain. Although these results are expected to control the magnetic anisotropy by the polarized femtosecond laser pulses, details are under investigation.

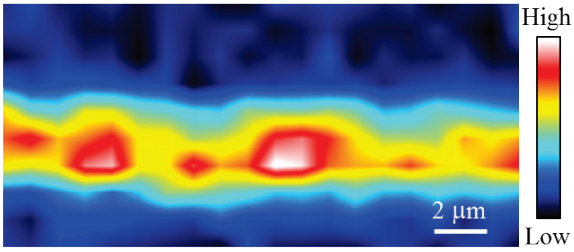

Fig. 6 Raman spectral map at 256 cm^{-1} peak intensity after the laser direct writing with a pulse energy of 1.5 μJ.

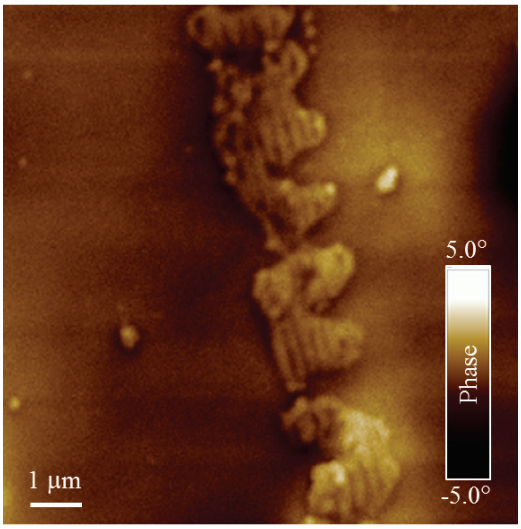

Fig. 7 Magnetic force microscope image on the surface polished to the depth of laser trace written by femtosecond laser with 1.5 μJ.

4. Conclusion

We have investigated the structure induced by femtosecond laser pulses in Al_2O_3-Dy_2O_3 binary glasses which were prepared by aerodynamic levitation method. We found that the structures depend on the laser pulse energy. In the condition of more than 1.3 μJ, nanogratings can be observed in SEM measurement and there was birefringence in modified region because of nanogratings in polarization microscope image. On the other hand, in the condition of less than 1.0 μJ, the formation of nanogratings were not perfect and birefringence which was attributed to nanogratings cannot be observed. Raman spectra measurements revealed that $Dy_3Al_2(AlO_4)_3$ crystals appeared along with the laser scanning. These results means the formation of nanogratings and crystallization occurred simultaneously when the laser beam was focused. MFM image indicated that magnetic domains, which are apparently similar to the nanogratings, exist.

Acknowledgments

This work was partially supported by JSPS KAKENHI Grant Number 26630129, The Thermal & Electric Energy Technology Foundation, Tokuyama Science Foundation, Cross-Ministerial Strategic Innovation Promotion (SIP) Program and Industry-Academia Collaborative R&D Programs (Super Cluster Program).

References

[1] Y. Shimotsuma, P.G. Kazansky, J. Qiu and H. Hirao: Phys. Rev. Lett., 91, (2003) 247405.
[2] M. Lancry, R. Desmarchelier, K. Cook, B. Paumellec and J. Canning: Micromachines, 5, (2014) 825.
[3] M. Lancry B. Poumellec, J. Canning, K. Cook, J. C. Poulin and F. Brisset: Laser Photonics Rev., 7, (2013) 953.
[4] M. Birnbaum: J. Appl. Phys. 36, (1965) 3688.
[5] J. Bonse, J. Krüger, S. Höhm and A. Rosenfeld: J. Laser Appl. 24, (2012) 042006.
[6] J. E. Sipe, J. F. Young, J. S. Preston and H. M. van Dri-el: Phys. Rev. B 27, (1983) 1141.
[7] Y. Shimotsuma, K. Hirao, J. Qiu and P. G. Kazansky: Mod. Phys. Lett. B 19, (2005) 225.
[8] S. Richter, C. Miese, S. Döring, F. Zimmermann, M. J. Withford, A. Tünnermann and S. Nolte: Opt. Mater. Express 3, (2013) 1161.
[9] V. R. Bhardwaj, E. Simova, P. P. Rajeev, C. Hnatovsky, R. S. Taylor, D. M. Rayner and P. B. Corkum: Phys. Rev. Lett. 96, (2006) 057404.
[10]L. Sudrie, M. Franco, B. Prade and A. Mysyrowicz: Opt. Common., 171, (1999) 279.
[11]J. D. Mills, P. G. Kazansky, E. Bricchi and J. J. Baumberg: Appl. Phys. Lett., 81, (2002) 196.
[12]E. Bricchi, B. G. Klappauf and P. G. Kazansky: Opt. Lett., 29, (2004) 119.
[13]C. Hnatovsky and R. S. Taylor: Appl. Phys. Lett. , 87, (2005) 014104.
[14]Y. Shimotsuma, M. Sakakura, P. G. Kazansky, M. Beresna, J. Qiu, K. Miura and K. Hirao: Adv. Mater., 22, (2010) 4039.
[15]Y. Shimotsuma, K. Miura and K. Hirao: Int. J. Appl. Glass Sci., 4, (2013) 182.
[16]M. Beresna, M. Gecevičius and P. G. Kazansky: Opt. Mater. Express 1, (2011) 783.
[17]A. Masuno, Y. Watanabe, H. Inoue, Y. Arai, J. Yu and M. Kaneko: Phys. Status Solidi C 9, 12, (2012) 2424.
[18]Y. Watanabe, A. Masuno and H. Inoue: J. Non-Cryst. Solids, 358, (2012) 3563.
[19]M. V. Kumar, T. Ishikawa, B. Basavalingu, J. T. Okada and Y. Watanabe: J. Appl. Phys., 113, (2013) 193503.
[20]H. Inoue, Y. Watanabe, A. Masuno, M. Kaneko and J. Yu: Opt. Mater., 33, (2011) 1853.
[21]K.J. Lee, W. S. Hwang, C. H. Lee, S. Yoda and W. S. Cho: Thermochimica Acta, 542, (2012) 37.
[22]A. Masuno and H. Inoue: Appl. Phys. Express, 3, (2010) 102601.
[23]A. Masuno, S. Kohara, A. C. Hannon, E. Bychkov and H. Inoue: Chem. Mater., 25, (2013) 3056.
[24]M. Born, E. Wolf: "Principles of Optics" (Pergamon Press, Oxford, 1968).
[25]T. Asai, Y. Shimotsuma, T. Kurita, A. Murata, S. Kubota, M. Sakakura, K. Miura, F. Brisset, B. Poumellec and M. Lancry: J. Am. Ceram. Soc., 98, (2015) 1471.
[26]L. Belliard, A. Thiaville, S. Lemerle, A. Lagrange, J. Ferré and J. Miltat: J. Appl. Phys. 81 (1997) 3849.

(Received: May 25, 2015, Accepted: January 24, 2016)